



OPEN

Comparison between biparametric and multiparametric MRI in predicting muscle invasion by bladder cancer based on the VI-RADS

Tae Il Noh¹, Ji Sung Shim¹, Sung Gu Kang¹, Deuk Jae Sung², Jun Cheon¹, Ki Choon Sim^{2,3}✉ & Seok Ho Kang^{1,3}✉

This study aimed to compare the diagnostic validity of biparametric magnetic resonance imaging (bpMRI) with that of multiparametric MRI (mpMRI) based on the Vesicle Imaging-Reporting and Data System (VI-RADS) in predicting muscle invasion by bladder cancer (BCa). We retrospectively examined 357 patients with an initial diagnosis of BCa who underwent preoperative MRI; 257 and 100 patients underwent mpMRI and bpMRI, respectively. Two urogenital radiologists evaluated all bpMRI and mpMRI scans using VI-RADS, and the diagnostic validity of VI-RADS for predicting muscle invasion by BCa was analyzed based on histopathology of the first and/or second transurethral resection of bladder tumors and radical cystectomy. Receiver operating characteristic (ROC) curves were plotted with the calculation of area under the curves (AUCs), and the level of significance was $P < 0.05$. Both groups showed optimal performance with a VI-RADS score ≥ 3 . BpMRI showed comparable diagnostic performance to mpMRI (reader 1: AUC, 0.903 [0.827–0.954] vs. 0.935 [0.884–0.968], $p = 0.510$; and reader 2: AUC, 0.901 [0.814–0.945] vs. 0.915 [0.874–0.946]; $p = 0.655$). The inter-reader agreement between both readers was excellent (Cohen's kappa value = 0.942 and 0.905 for bpMRI and mpMRI, respectively). This comparative study suggests that bpMRI has comparable diagnostic performance to mpMRI and may be an alternative option to predict muscle invasion by BCa.

Abbreviations

ADC	Apparent diffusion coefficient
AUC	Area under the ROC curve
BCa	Bladder cancer
BP	Biparametric
bpMRI	Biparametric MRI
CM	Contrast media
DCE	Dynamic contrast enhanced
DW	Diffusion-weighted category
DWI	Diffusion weighed imaging
HG	High grade
MIBC	Muscle invasive bladder cancer
MP	Multiparametric
mpMRI	Multiparametric MRI
MRI	Magnetic resonance imaging
NMIBC	Non-muscle invasive bladder cancer
RC	Radical cystectomy
ROC	Receiver-operating characteristic

¹Department of Urology, Anam Hospital, Korea University College of Medicine, 73 Goryeodae-Ro, Seongbuk-Gu, Seoul 02841, Korea. ²Department of Radiology, Anam Hospital, Korea University College of Medicine, Seoul, Korea. ³These authors contributed equally: Ki Choon Sim and Seok Ho Kang. ✉email: ha2sky@hanmail.net; mdksh@korea.ac.kr

SC	Structural category
SI	Signal intensity
TURBT	Transurethral resection of bladder tumor
T2WI	T2-weighted imaging
VI-RADS	Vesicle Imaging-Reporting and Data System

Bladder cancer (BCa) is among the most commonly diagnosed cancers worldwide; it comprises 3% of all newly diagnosed cancers and is 3.4 times more common in men than in women¹. BCa is classified as non-muscle invasive BCa (NMIBC) or muscle invasive BCa (MIBC) depending on whether the muscularis has been invaded². Approximately 20–25% of newly diagnosed BCAs are MIBCs. Moreover, approximately 70% of patients experience NMIBC recurrence even after initial treatment with transurethral resection of a bladder tumor (TURBT). Of these patients, 10–20% experience progression to MIBC³.

The surgical management and prognoses of NMIBC and MIBC are entirely different from each other⁴. Although the recommendations for BCAs are established based on complex clinical, pathological, and imaging factors, the treatments are based on local staging primarily with specimens obtained by TURBT. For NMIBCs, TURBT with or without intravesical therapy has been used as a primary treatment to reduce recurrence and progression to MIBC⁵. Contrastingly, for MIBCs, which demonstrate the invasion of the muscularis propria layer in TURBT, radical cystectomy (RC) with lymph node dissection is the surgical standard. Even postoperatively, chemotherapy and radiotherapy are required for unfit patients undergoing RC, due to the aggressiveness and poor prognosis of MIBC⁶. Therefore, it is essential to confirm the local stage to decide treatment strategies. For all tumors diagnosed as T1 high grade (HG), as well as those not including the detrusor muscle in the specimen, a second look and repeated TURBT (re-TURBT) are recommended^{5,7}.

However, since re-TURBT has a risk of complications, including bleeding and bladder wall perforation⁸, magnetic resonance imaging (MRI) without radiation is being increasingly considered for the staging of BCa as the modality of choice for imaging. The Vesical Imaging-Reporting and Data System (VI-RADS), a multiparametric MRI (mpMRI) reporting system for BCa staging and muscle invasion prediction, has recently been launched⁸. It shows high sensitivity, specificity, and accuracy for predicting the invasiveness of bladder tumors in the muscle layer^{9,10}.

The guidelines of the European Association of Urology (EAU) recommend the inclusion of multiplanar T2-weighted imaging (T2WI), diffusion-weighted imaging (DWI), and dynamic contrast-enhanced (DCE) MRI in a mpMRI protocol for VI-RADS scoring⁶.

Although a contrast-free protocol is a relatively novel topic in the literature for BCa, our study was prompted by the question of whether the contrast material, considering its side effects, is truly essential in predicting muscle invasion. Only a few studies with a small sample size have compared the diagnostic performance between biparametric MRI (bpMRI) and mpMRI; both imaging modalities had similar sensitivity and specificity^{11–15}. The present study aimed to validate the use of VI-RADS in patients with BCa and compare its diagnostic performance for predicting muscle invasion between two different protocols: bpMRI and mpMRI. Herein, we investigated whether contrast media is essential and whether contrast-free bpMRI without a DCE sequence can be considered an alternative to standard mpMRI.

Materials and methods

Study population and design. We retrospectively examined 357 patients between January 2018 and June 2021 with an initial diagnosis of BCa who underwent preoperative MRI; 257 and 100 patients underwent mpMRI and bpMRI, respectively.

Inclusion criteria were as follows: (1) patients with suspected bladder mass on computed tomography (CT) and/or cystoscopy examination; (2) patients who underwent bpMRI or mpMRI using a 3.0-T scanner; and (3) patients with subsequent TURBT-proved urothelial BCa. Exclusion criteria were as follows: (1) patients who underwent biopsy alone due to unfit for proper TURBT (mpMRI group, $n = 4$; and bpMRI group, $n = 1$); and (2) patients who had severe susceptibility artifacts in the pelvis (i.e., hip joint replacement) (mpMRI group, $n = 2$).

Between January 2018 and December 2018, a predetermined number ($n = 100$) of patients with BCa satisfying the inclusion/exclusion criteria underwent bpMRI, which was performed before mpMRI with a DCE sequence was recommended and adopted in our institution. After the adoption of VI-RADS, 257 patients with BCa satisfying the inclusion/exclusion criteria between January 2019 and June 2021 underwent mpMRI. The endpoint of this study was to compare the diagnostic performance of mpMRI with that of bpMRI in predicting MIBC.

mpMRI and bpMRI examinations. Patients were prepared according to the guidelines of the EAU⁸ and Sim et al.'s method¹⁶. All MRI examinations were performed using 3.0-T equipment (Magnetom Skyra and Prisma, Siemens Healthineers, Erlangen, Germany or Achieva, Philips Healthcare, Best, Netherlands) and a multichannel phased-array external surface coil. The entire pelvis was imaged from the aortic bifurcation to the inferior margin of the pubic symphysis. High-resolution fast spin-echo nonfat-suppressed T2-weighted images in three orthogonal planes were obtained. DWI was performed during free breathing using a water-excited single-shot spin-echo echo-planar sequence in the axial planes. DCE MR images were acquired using an axial fat-suppressed three-dimensional volumetric spoiled gradient-echo sequence before and after intravenous injection of 0.2 mL/kg of gadotrate meglumine (Dotarem; Guerbet) at 2 mL/s, up to a total volume of 20 mL. Four sets of contrast-enhanced images were obtained 30–120 s after contrast material injection. The detailed MRI protocols are summarized in Supplemental Table 1.

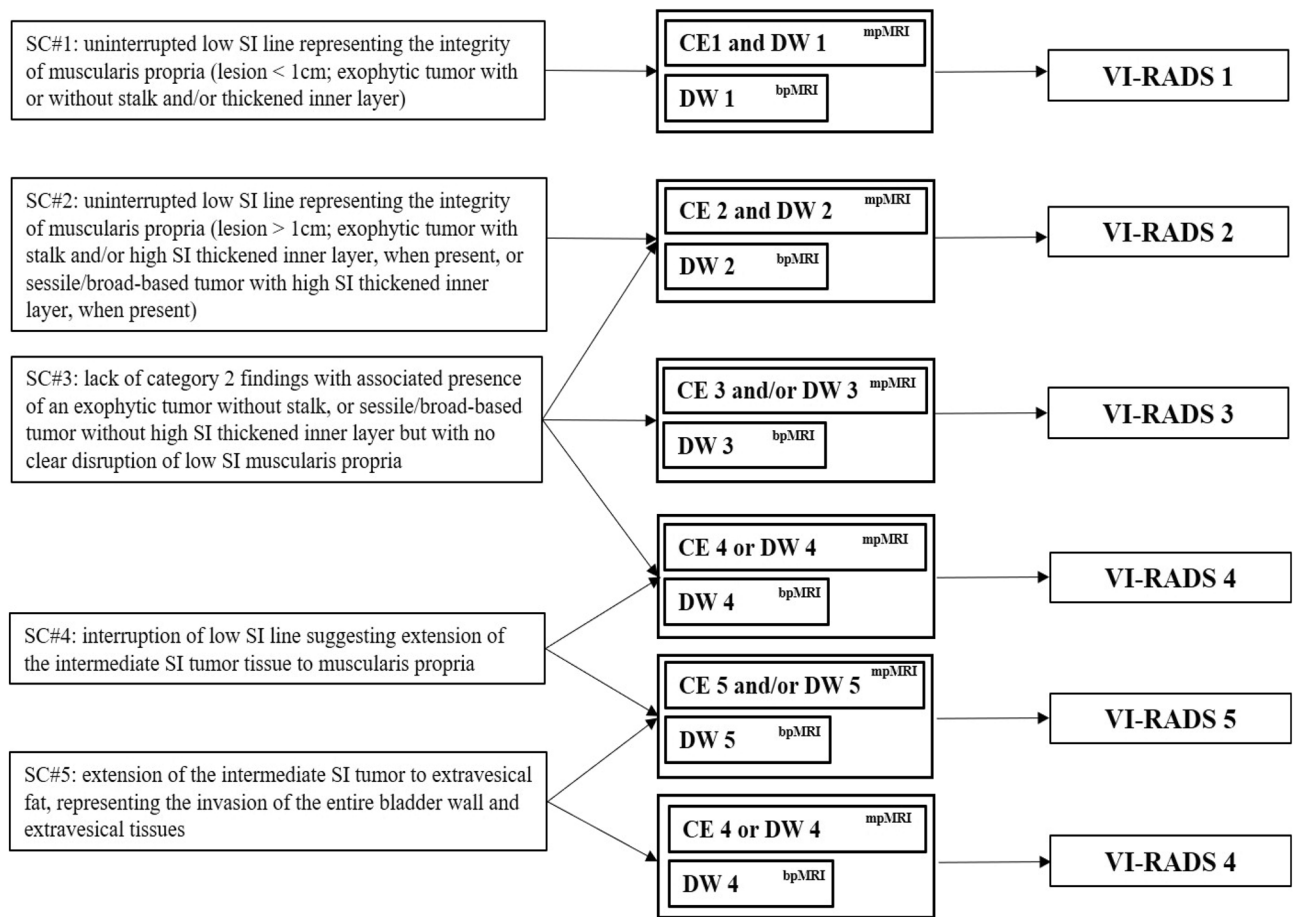


Figure 1. Summary of the schematic representation of the bp- and mpVI-RADS scoring interpretation. A five-point biparametric VI-RADS (bpVI-RADS) score is generated using the individual T2WI and DWI. The T2-weighted sequence is the dominant sequence, and the diffusion-weighted sequence is considered as a first pass guide. For categories 1–3, the “first pass scoring” T2 sequence should be considered. For categories 4 and 5, the dominant sequences (i.e., when image quality is optimal) are present in DWI for bpVI-RADS, DWI (first) and DCE (second; especially if the DWI is suboptimal) for mpVI-RADS. *bpMRI* biparametric MRI, *DW* diffusion-weighted category, *DWI* diffusion-weighted imaging, *mpMRI* multiparametric MRI, *SC* structural category, *SI* signal intensity, *VI-RADS* Vesicle Imaging-Reporting and Data System.

MR image interpretation. For comparison between MRI images, two urogenital radiologists with > 10 years of experience through separate sessions evaluated all bpMRI and mpMRI scans using the VI-RADS classification system (Fig. 1). The reviewers were blinded to the clinical, surgical, and histopathological results associated with the images. All lesions were scored separately according to the VI-RADS criteria using images obtained via T2WI, DWI, and/or DCE MRI. The VI-RADS score reflecting the overall risk score of detrusor muscle invasion for each patient was assigned as described in the literature according to the following findings⁸:

T2WI: Interruption of the hypointense line of the muscle layer by a tumor with T2 intermediate signal intensity or extension of the tumor to the extravesical fat.

DWI: Extension of a hyperintense tumor on DWI and low signal intensity on an apparent diffusion coefficient (ADC) map to the hypointense line of the muscle layer or extravesical fat.

DCE: Extension into the hypointense line of the muscle layer by early enhancement of the tumor or the tumor stalk not being observed.

The VI-RADS scores are as follows⁸:

VI-RADS score 1: Uninterrupted low SI line representing muscularis integrity (size, < 1.0 cm).

VI-RADS score 2: Similar to VI-RADS score 1, except for a size > 1.0 cm and a thickened inner layer.

VI-RADS score 3: Disappearance of category 2 findings, but no clear disruption of low SI muscularis layer.

VI-RADS score 4: Interruption of low SI line suggesting extension into the muscularis layer.

VI-RADS score 5: Extension of the intermediate SI tumor to extra-vesical fat.

The schematic representation and scoring of VI-RADS for bpMRI are as follows (Figs. 1 and 2):

VI-RADS 1 (muscle invasion is highly unlikely): SC and DW category 1.

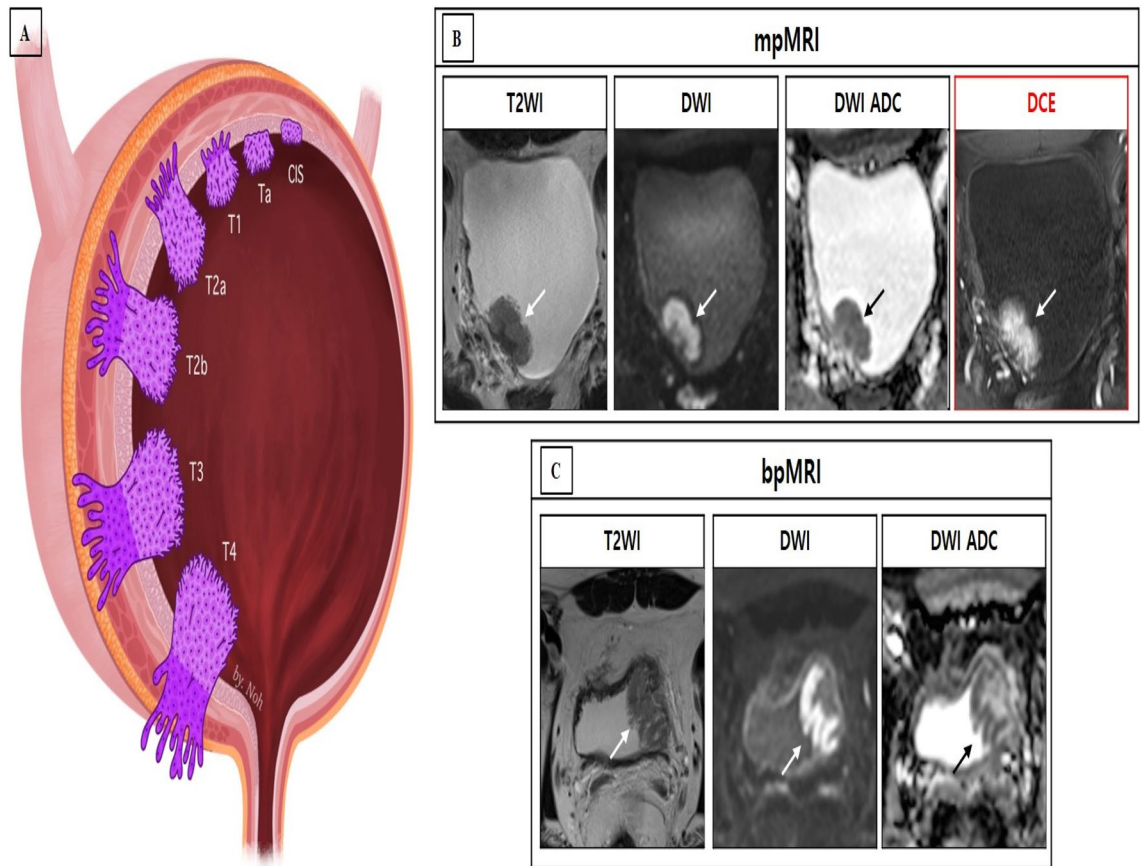


Figure 2. Schematic representation of the bladder cancer stage and case presentation of the VI-RADS scoring. **(A)** Bladder wall anatomy and local bladder tumor staging. **(B)** Multiparametric MRI (mpMRI) in a 63-year-old man. The bladder tumor was categorized as SC 4, DW 3, and CE 4 in axial T2-weighted magnetic resonance image (T2WI), diffusion-weighted image (DWI) with a high b value and apparent diffusion coefficient map (ADC), and dynamic contrast enhanced image (DCE) obtained 30 s after the administration of contrast material, respectively. The VI-RADS score was 4, and urothelial carcinoma (stage T2) was confirmed by the transurethral resection of bladder tumor (TURBT). **(C)** Biparametric MRI (bpMRI) in a 60-year-old man. The bladder tumor was categorized as SC 3 and DW 2 in axial T2WI and DWI with a high b value and ADC respectively. The VI-RADS was 2, and urothelial carcinoma (stage T1) was confirmed by TURBT. ADC apparent diffusion coefficient, DCE dynamic contrast enhanced, T2WI T2-weighted imaging, VI-RADS Vesicle Imaging-Reporting and Data System.

VI-RADS 2 (muscle invasion is unlikely): SC and DW category 2; and SC category 3 with DW category 2. In VI-RADS score 2, muscle invasion is unlikely.

VI-RADS 3 (presence of muscle invasion is equivocal): SC and DW category 3.

VI-RADS 4 (muscle invasion is likely): At least SC and/or DW category 4; SC category 3 with DWI category 4; and SC category 5 with DW category 4.

VI-RADS 5 (invasion of muscle and beyond the bladder is very likely): SC and DW category 5.

Standard of reference. TURBT was performed for all lesions of suspected BCa by a single surgeon with 15 years of experience and performed surgeries in > 200 cases of TURBTs and 50 cases of intracorporeal robot-assisted radical cystectomy with urinary diversion annually, amassing a total of 300 cases.

Re-TURBT was performed for tumors diagnosed as T1 HG tumors; this classification does not guarantee appropriate resection of all tumors and does not include the detrusor muscle in the specimen after primary TURBT. Subsequently, RC was performed in patients diagnosed with T1 HG (Bacillus Calmette–Guerin [BCG] unresponsive), T2, or higher-grade tumors. The histopathologic results of TURBT, re-TURBT, and RC performed by a single surgeon were used as the standard reference. The specimens were evaluated for the presence of muscle invasion by a dedicated uropathologist with 10 years of experience and blinded to MRI findings during evaluation. Tumor-node-metastasis staging and tumor grade were classified according to the World Health Organization class standards¹⁷.

Statistical analysis. To quantify and compare the discriminatory accuracy of each modality for identifying the muscle invasiveness of BCa, receiver operating characteristic (ROC) curve analyses were performed, and the results were summarized as the areas under the ROC curves (AUCs) and 95% confidence intervals (CIs). The

Variable (%)	Multiparametric MRI						Biparametric MRI					
	Total	VI-RADS 1	VI-RADS 2	VI-RADS 3	VI-RADS 4	VI-RADS 5	Total	VI-RADS 1	VI-RADS 2	VI-RADS 3	VI-RADS 4	VI-RADS 5
Number	257	28 (10.9)	147 (57.2)	31 (12.1)	20 (7.7)	31 (12.1)	100	18 (18.0)	49 (49.0)	13 (13.0)	8 (8.0)	12 (12.0)
Age (year), mean \pm SD	68.5 (12.5)						69.2 (11.5)					
Sex												
Male	217 (84.4)	23 (8.9)	127 (49.4)	28 (10.9)	19 (7.4)	21 (8.2)	84 (84.0)	15 (15.0)	40 (40.0)	12 (12.0)	8 (8.0)	9 (9.0)
Female	40 (15.6)	5 (1.9)	21 (8.2)	3 (1.2)	1 (0.4)	10 (3.9)	16 (16.0)	3 (3.0)	9 (9.0)	1 (1.0)	0 (0.0)	3 (3.0)
No. of lesions												
Unifocal	136 (52.9)	19 (7.4)	74 (28.8)	16 (6.2)	12 (4.7)	9 (3.5)	59 (59.0)	16 (16.0)	26 (26.0)	8 (8.0)	2 (2.0)	9 (9.0)
Multifocal	121 (47.1)	9 (3.5)	71 (27.6)	11 (4.3)	8 (3.1)	22 (8.6)	41 (41.0)	2 (2.0)	23 (23.0)	5 (5.0)	6 (6.0)	2 (2.0)
Diameter of index lesion size												
< 1 cm	28 (10.9)	28 (10.9)	0 (0.0)	0 (0.0)	0 (0.0)	0 (0.0)	18 (18.0)	18 (18.0)	0 (0.0)	0 (0.0)	0 (0.0)	0 (0.0)
1–3 cm	134 (52.1)	0 (0.0)	111 (43.2)	17 (6.6)	4 (1.6)	2 (0.8)	44 (44.0)	0 (0.0)	34 (34.0)	7 (7.0)	2 (2.0)	1 (1.0)
> 3 cm	95 (37.0)	0 (0.0)	36 (14.0)	14 (5.4)	16 (6.2)	29 (11.3)	38 (38.0)	0 (0.0)	15 (15.0)	6 (6.0)	6 (6.0)	11 (11.0)
T stage												
Tis	2 (0.8)	1 (0.4)	1 (0.4)	0 (0.0)	0 (0.0)	0 (0.0)	2 (2.0)	1 (1.0)	1 (1.0)	0 (0.0)	0 (0.0)	0 (0.0)
Ta	96 (37.4)	19 (7.4)	69 (26.8)	8 (3.1)	0 (0.0)	0 (0.0)	34 (34.0)	14 (14.0)	16 (16.0)	4 (4.0)	0 (0.0)	0 (0.0)
T1	90 (35.0)	8 (3.1)	66 (35.7)	11 (4.3)	5 (1.9)	0 (0.0)	40 (40.0)	3 (3.0)	28 (28.0)	6 (6.0)	3 (3.0)	0 (0.0)
\geq T2	69 (26.8)	0 (0.0)	11 (4.3)	12 (4.7)	15 (5.8)	31 (12.1)	24 (24.0)	0 (0.0)	4 (4.0)	3 (3.0)	5 (5.0)	12 (12.0)
Concomitant CIS	94 (37.0)	10 (3.9)	56 (21.8)	11 (4.3)	9 (3.5)	8 (3.1)	37 (37.0)	4 (4.0)	20 (20.0)	5 (5.0)	3 (3.0)	5 (5.0)
Pathology grade												
Low	46 (17.9)	10 (3.9)	29 (11.3)	7 (2.7)	0 (0.0)	0 (0.0)	22 (22.0)	9 (9.0)	10 (10.0)	3 (3.0)	0 (0.0)	0 (0.0)
High	211 (82.1)	16 (6.2)	117 (45.5)	24 (9.3)	20 (7.8)	31 (12.1)	78 (78.0)	8 (8.0)	39 (39.0)	10 (10.0)	8 (8.0)	12 (12.0)
re-TURBT	49 (54.4)	6 (75.0)	33 (50.0)	8 (72.7)	1 (20.0)	0 (0.0)	15 (37.5)	1 (33.3)	9 (32.1)	2 (33.3)	3 (100.0)	0 (0.0)
Upstage	2 (4.1)	0 (0.0)	1 (3.0)	1 (12.5)	0 (0.0)	0 (0.0)	1 (6.7)	0 (0.0)	0 (0.0)	1 (50.0)	0 (0.0)	0 (0.0)
Cystectomy	43 (16.7)	0 (0.0)	10 (3.9)	8 (3.1)	9 (3.5)	16 (6.2)	20 (20.0)	0 (0.0)	4 (4.0)	3 (3.0)	4 (4.0)	9 (9.0)
MRI												
Scan time (SD), min	35.3 (5.7)						24.4 (4.2)					
Cost (SD), USD	1320 (23.2)						1073 (15.4)					

Table 1. Characteristics of patients with bladder cancer lesions using VI-RADS. Percentages are presented in parentheses. CIS carcinoma in situ, VI-RADS Vesical Imaging Reporting and Data System, re-TURBT repeated transurethral resection of a bladder tumor, Tis carcinoma in situ, Ta noninvasive papillary carcinoma, T1 tumor invades subepithelial connective tissue, T2 tumor invades muscular propria, MRI magnetic resonance imaging, SD standard deviation, USD United States dollar.

VI-RADS cut-off were determined by the ROC curves analysis by Youden's index. The sensitivity and specificity of the cut-off value of each VI-RADS score were determined using a 2 \times 2 contingency table. Descriptive statistics were calculated using VI-RADS \geq 3 as the cut-off for muscle invasion by BCa (Supplemental Table 2). For each reader, the ROC curves were computed for bpMRI and mpMRI, and a pairwise comparison of AUCs was performed using Delong's test. Inter-reader agreement between readers 1 and 2 was assessed using Cohen's Kappa statistics.

All statistical analyses were performed using IBM SPSS version 24.0 (IBM Corp., Armonk, NY, USA) and R software version 3.6.1 (R Foundation for Statistical Computing, Vienna, Austria). A p-value < 0.05 was considered statistically significant.

Ethics statement. This study was conducted according to the guidelines of the Declaration of Helsinki and current ethical guidelines. The study was reviewed and approved by the Ethics Committee and Institutional Review Board of the Korea University Anam Hospital (IRB No. 2019AN0360). Written informed consent was obtained from all study participants prior to their enrolment.

Results

The total number of BCas analyzed was 357, with 100 patients undergoing bpMRI and 257 undergoing mpMRI. Table 1 shows the characteristics of both groups, with the bpMRI group including 84 men and 16 women aged 69.2 \pm 11.5 years and the mpMRI group including 217 men and 40 women aged 68.5 \pm 12.5 years. All patients underwent TURBT [bpMRI group: NMIBC, 76 (76.0%, more in detail; Tis, 2; Ta, 34; and T1:40) and MIBC, 24 (24.0%); mpMRI group: NMIBC, 188 (73.2%, more in detail; Tis, 2; Ta, 96; and T1:90) and MIBC, 69 (26.8%)].

VI-RADS ≥ 3	Reader 1			Reader 2		
	bpMRI	mpMRI	P value	bpMRI	mpMRI	P value
Sensitivity (95% CI)	83.3 (62.6–95.3)	86.8 (71.9–95.6)	0.405	82.6 (61.2–95.0)	83.9 (72.3–92.0)	0.512
Specificity (95% CI)	82.4 (71.8–90.4)	93.3 (87.2–97.1)	0.048	81.8 (71.4–89.7)	89.1 (83.8–93.1)	0.108
AUC (95% CI)	0.903 (0.827–0.954)	0.935 (0.884–0.968)	0.510	0.901 (0.814–0.945)	0.915 (0.874–0.946)	0.655

Table 2. Diagnostic performance between both readers in predicting muscle invasion by bladder cancer. *AUC* area under the curve, *bpMRI* biparametric magnetic resonance imaging, *mpMRI* multiparametric magnetic resonance imaging, *VI-RADS* Vesical Imaging Reporting and Data System, *CI* confidence interval.

In the bpMRI group, 15 of 40 (37.5%) patients underwent re-TURBT, and upstaging from T1 to T2 in the re-TURBT group was confirmed in 1 of 15 patients (6.7%), who was 1 of the 8 patients with VI-RADS 3 score in the re-TURBT group. In the mpMRI group, 49 of 90 (54.4%) patients underwent re-TURBT, and upstaging from T1 to T2 in the re-TURBT group was confirmed in 2 of 49 (4.1%) patients in the re-TURBT group.

The rates of muscle invasion were 8.2% and 7.5% for VI-RADS score 2, 23.1% and 38.7% for VI-RADS score 3, 62.5% and 75.0% for VI-RADS score 4, and 100% and 100% for VI-RADS score 5 groups for bpMRI and mpMRI, respectively. RC was performed following TURBT in 20 of 100 (20.0%) cases in the bpMRI group and in 43 of 257 (16.7%) cases in the mpMRI group. The mean acquisition time was shorter in bpMRI than in mpMRI [bpMRI, 24.4 ± 4.2 min (mean \pm SD); and mpMRI 35.3 ± 5.7 min (mean \pm SD) ($p = 0.045$)]. The cost \pm SD for bpMRI and mpMRI were US\$1,073 (15.4) and US\$1,320 (23.2), respectively.

BpMRI showed optimal performance with a VI-RADS score ≥ 3 as follows: reader 1, sensitivity (95% CI): 83.3% (62.6%–95.3%) and specificity: 82.4% (71.8%–90.4%); and reader 2, sensitivity (95% CI): 82.6% (61.2%–95.0%) and specificity: 81.8% (71.4%–89.7%). mpMRI also showed an optimal performance with a cut-off of VI-RADS score ≥ 3 as follows: reader 1, sensitivity (95% CI): 86.8% (71.9%–95.6%) and specificity: 93.3% (87.2%–97.1%); and reader 2, sensitivity (95% CI): 83.9% (72.3%–92.0%) and specificity: 89.1% (83.8%–93.1%). VI-RADS score ≥ 3 was assumed to define MIBC, and the ROC curves were constructed accordingly. The AUCs (95% CI) of bpMRI and mpMRI with the criterion of VI-RADS score ≥ 3 were comparable (reader 1: 0.903 [0.827–0.954] vs. 0.935 [0.884–0.968], $p = 0.510$; and reader 2: 0.901 (0.814–0.945) and 0.915 (0.874–0.946), $p = 0.655$, in bpMRI vs. mpMRI, respectively) (Table 2, Fig. 3).

There was excellent inter-reader agreement between readers 1 and 2 in the VI-RADS scores using bpMRI and mpMRI, and the agreement value (Cohen's kappa value) of both readers was 0.942 and 0.905 for bpMRI and mpMRI, respectively.

Discussion

The treatment method for BCa can be determined based on complex factors such as stage, tumor grade, subtype of histopathology, and response to intravesical therapies such as BCG and chemotherapeutic agents⁵. However, one of the primary considerations regarding decisions for the prognosis and management of BCa is the local tumor stage. Although BCa staging is established based on a combination of clinical, pathological, and imaging methods, the local tumor stage is primarily determined according to the presence or absence of muscle invasion based on pathological specimens obtained by TURBT⁶.

The main framework of treatment is completely different depending on the presence or absence of muscle invasion. Therefore, predicting muscle invasion is essential in determining treatment; re-TURBT is recommended for confirming the presence of muscle invasion for all T1 HG tumors, as well as tumors in which no muscularis propria is included in the specimen⁷.

Primary TURBT may be inadequate, with a high percentage of residual tumors (33%–76%) and a high upstaging rate (0%–32%) after re-TURBT. Re-TURBT has been recommended as a second-look procedure for residual tumors and the confirmation of the presence of the muscularis propria; however, re-TURBT has a risk of possible complications such as perforation and bleeding¹⁸.

To reduce the potential risks of re-TURBT, radiologic imaging has been proposed to discriminate MIBCs from NMIBCs. Both CT and mpMRI are available for the diagnosis and assessment of stages of local BCa before TURBT according to the guidelines of the EAU⁶. For the detection and staging of BCa, CT urography is generally performed. However, this method has its own drawbacks in predicting muscle invasion by BCa¹⁹. To distinguish MIBCs from NMIBCs, VI-RADS with MRI was developed, and published literature has demonstrated its clinical reliability^{20–22}. With the guarantee of appropriate tumor resection by an experienced surgeon and no suspicion of muscle invasion on MRI with VI-RADS, re-TURBT could be omitted and avoided²³.

Furthermore, MRI based on VI-RADS has the perspective applicability to be broadly used for follow-up in patients with BCa²³. Two potential applications of MRI based on VI-RADS are assessment of responses to systematic therapy and risk assessment²⁴ and active surveillance. Active surveillance may be considered in patients with low risk NMIBC²⁵. To reduce the potential risk of surgical management and discomfort from frequent cystoscopy following TURBT, an alternative tool using a regression algorithm (Xpert Bladder Monitor Test) for active surveillance has also been reported²⁶. As T2WI MRI provides optimal soft-tissue contrast, mpMRI for the standardized discrimination of MIBCs from NMIBCs and its potential applications are promising. However, some possible drawbacks, such as mpMRI being time consuming and costly²⁷ and the potential risks associated with the contrast media, such as contrast-induced nephropathy including nephrogenic systemic fibrosis, renal insufficiency, renal failure, and the accumulation of gadolinium, should be considered^{28,29}. The incidence rate

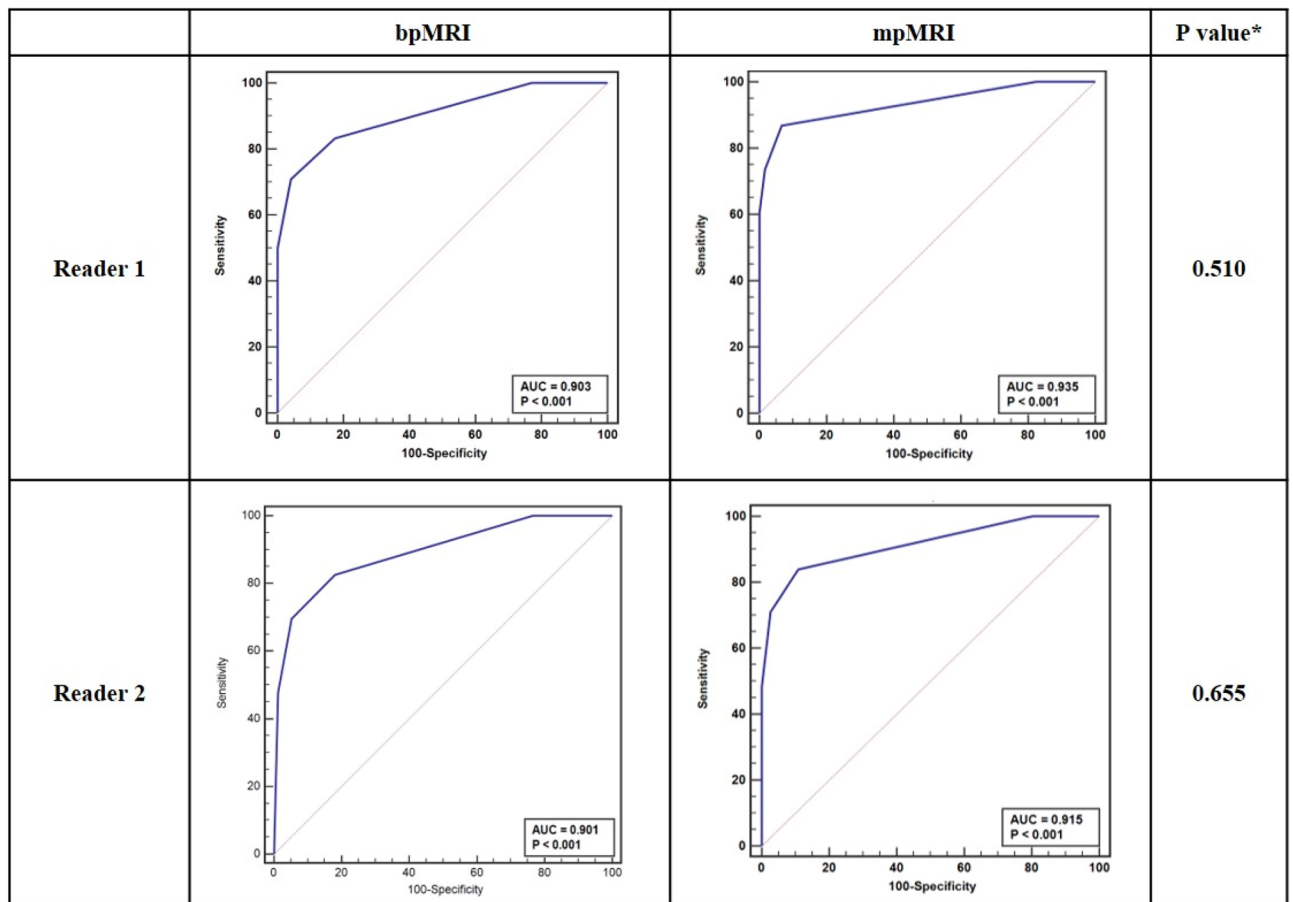


Figure 3. Comparison of ROC curve and inter-reader agreement between bpMRI and mpMRI. A VI-RADS score ≥ 3 was assumed to define MIBC. Asterisk: comparison of two independent ROC curves between bpMRI and mpMRI was performed using Delong's test. *AUC* area under the curve, *bpMRI* biparametric magnetic resonance imaging, *mpMRI* multiparametric magnetic resonance imaging, *ROC* receiver operating characteristics.

of contrast media-induced nephropathy ranged from 0.15%–2.0%, is related to an increase of $\geq 25\%$ in serum creatinine levels, and is responsible for approximately 10% of cases of hospital-acquired acute renal failure in Europe and the United States^{30,31}. To overcome these drawbacks of mpMRI, several alternative imaging tools have been proposed. One noteworthy imaging tool is the high-resolution microultrasound imaging proposed for BCa detection and staging³², which shows an excellent performance compared to that of mpMRI³³. However, as high-resolution microultrasound imaging is still limited owing to the lack of equipment availability and expertise necessary, a significant learning curve related to the use of high-resolution microultrasound techniques is required³³. Therefore, we focused on bpMRI, a contrast-free protocol based on the standardized reporting system (VI-RADS), and compared the diagnostic performance between bpMRI and mpMRI. In this study, the protocols of both bpMRI and mpMRI showed high performance, with an AUC of over 0.90. Moreover, VI-RADS has been demonstrated to be a promising predictor of muscle invasion with good reproducibility. While retaining sufficient diagnostic performance, bpMRI showed superiority in the time and cost analyses compared to mpMRI.

The value of a contrast-free protocol in BCa is a relatively novel topic; however, such a protocol has been investigated in prostate cancer based on the Prostate Imaging Reporting & Data System score, and bpMRI has shown a diagnostic performance comparable to that of mpMRI for clinically significant prostate cancer detection^{34,35}.

In a study with 54 patients with BCa, bpMRI and mpMRI had comparable diagnostic accuracy in predicting MIBC, with no statistically significant differences in AUCs [reader 1: 0.985 (0.912–0.998) vs. 0.968 (0.884–0.996), $p = 0.154$; reader 2: 0.942 (0.846–0.986) and 0.936 (0.839–0.983), $p = 0.345$; and reader 3: 0.945 (0.848–0.986) and 0.935 (0.838–0.983), $p = 0.338$, in bpMRI vs. mpMRI, respectively]¹³. Moreover, the inter-reader agreement of VI-RADS was good for both bpMRI (k range, 0.814–0.86) and mpMRI (k range, 0.787–0.859)¹³. Furthermore, in a meta-analysis of 10 studies on mpMRI and 7 studies on mpMRI/bpMRI comprising \geq VI-RADS 3 as the cut-off, the sensitivities of bpMRI and mpMRI were not significantly different ($p = 0.15$), yet bpMRI was more specific [0.90 (0.81–0.95) vs. 0.86 (0.77–0.91), $p = 0.02$, in bpMRI vs. mpMRI]³⁶.

Non-contrast-enhanced MRI with only a fused high b-value DWI/ADC map and T2WI may be a promising method for assessing the depth of invasion in patients with BCa³⁷. Accordingly, the issues regarding the

contrast-free protocol comprise several questions regarding the major role of contrast media. It is necessary to look at each of the major roles of T2WI, DWI, and DCE sequences in predicting muscle invasion.

T2WI provides optimal soft-tissue contrast. On T2WI, the hypointense band of the muscularis propria layer is well distinguished against a marked hyperintense signal of urine and perivesical fat, including an intermediate intensity signal of the bladder tumor. Therefore, T2WI could be a key sequence for predicting muscle invasion¹⁶. DWI has inherent drawbacks of a low signal-to-noise ratio and spatial resolution³⁸. Thus, DWI is vulnerable to disturbance by various artifacts, and its role is limited for the evaluation of small tumors and differentiation of tumors from benign conditions. To compensate for these inherent drawbacks of DWI, DCE may be considered to ensure the proper interpretation of the lesion. On a DCE sequence, tumors show rapid enhancement by contrast media, which could help distinguish tumors from the muscularis propria³⁹. DCE may increase accuracy and reduce false negatives more than DWI alone. Moreover, the diagnostic performance of radiologists is not significantly affected by DCE³⁶. However, DCE imaging in addition to DWI has been reported to induce a worse diagnostic performance in less experienced radiologists¹⁴.

Urologists establish treatment strategies for BCa based on a combination of clinical, pathological, and imaging factors through multi-modal approaches, including MRI and TURBT⁵. MRI is useful as an adjuvant tool but cannot replace tumor grading defined by TURBT²³. Furthermore, in this study, bpMRI showed a comparable performance to mpMRI in predicting muscle invasion by BCa. Therefore, the need to add a DCE sequence to predict MIBC, with the potential risk of contrast media, is limited and uncertain.

The contrast-free protocol of bpMRI reduces the potential risks associated with intravenous contrast media. The preservation of renal function may be related to the prognosis of BCa for several reasons. First, the median age at first diagnosis is approximately 70 years, with a relatively high risk of underlying renal disease and decreased renal function⁴⁰. Second, cisplatin-based chemotherapy, which requires eligible renal function (≥ 60 mL/min), is recommended as a basic chemotherapeutic treatment for MIBC⁶. Third, renal function can be compromised by the aggressive nature of bladder tumors, including conditions such as hydronephrosis and obstructive nephropathy⁴¹. Furthermore, the purpose of MRI for BCa is to predict MIBCs and follow the response to neoadjuvant or adjuvant chemotherapy; however, repeated intravenous contrast injection can affect renal function. Thus, the preservation of renal function should be considered in the management of BCa. Other benefits of avoiding DCE with contrast media include a shorter MRI scan time, improved patient comfort, no worries of contrast allergy, and reduced cost⁴².

The results of the present study demonstrate that VI-RADS is reliable and reproducible for predicting muscle invasiveness, regardless of the MRI protocol. Furthermore, bpMRI is more advantageous than the contrast-enhanced protocol, all while retaining diagnostic performance despite the absence of DCE sequences. Therefore, bpMRI could be a cost-effective alternative for predicting the muscle invasiveness of BCa.

However, to the best of our knowledge, only a few studies have compared DWI and DCE sequences for VI-RADS assessment, and most had a small sample size^{11–15}. Furthermore, the authors of previous studies only compared the performance of DWI and DCE in the same patients who underwent mpMRI, not contrast-free bpMRI. DWI and DCE were separated from the same mpMRI images, and VIRADS scoring was performed based on reference to each separated sequence. Two sets of images from the same BCa patients, set 1 (T2 plus DWI) also showed comparable high performance to set 2 (T2 plus DWI plus DCE) (AUC ranged between 0.90 and 0.95 and 0.87–0.95 for bpMRI and mpMRI, $P > 0.05$)^{11,14}. In a comparison study between bpMRI and mpMRI comprising 176 different patients (mpMRI, $n = 97$; and bpMRI, $n = 79$), the AUCs of VI-RADS using bpMRI and mpMRI were 0.88 and 0.84, respectively¹⁵. However, in meta-regression analyses, the number of patients (> 205 vs. ≤ 205), magnetic field strength (3.0 vs 1.5 T), and VI-RADS cut-off score (≥ 3 vs. ≥ 4) were significant factors affecting performance ($p \leq 0.03$)⁹.

Therefore, the strengths of this study were the comparison between bpMRI and mpMRI with 3.0-T equipment and VI-RADS cut-off score ≥ 3 , rather than a comparison between DWI and DCE sequences in the same patient. Moreover, the current study comprises an appropriately large sample size ($n = 357$) with excellent inter-reader agreement between two expert urogenital radiologists. Nevertheless, this study has the inherent limitations of its retrospective study design related to the heterogeneity of enrolled patients, as well as the selection and attrition biases. Therefore, well-designed randomized trials are needed to establish the utilization of bpMRI for predicting the muscle invasiveness of BCa.

Conclusions

The current comparison between bpMRI and mpMRI in predicting muscle invasion by BCa suggests that bpMRI has a comparable performance to mpMRI while retaining the advantages of a contrast-free protocol. Therefore, bpMRI may be a cost-effective alternative for predicting the muscle invasiveness due to BCa.

Data availability

All data generated or analyzed during this study are included in this article and its supplementary information files. The datasets used and/or analyzed in this study are available from the corresponding author upon reasonable request.

Received: 21 February 2022; Accepted: 26 August 2022

Published online: 30 November 2022

References

1. Bray, F. *et al.* Global cancer statistics 2018: GLOBOCAN estimates of incidence and mortality worldwide for 36 cancers in 185 countries. *CA Cancer J. Clin.* **68**, 394–424 (2018).

2. Soukup, V. *et al.* Prognostic performance and reproducibility of the 1973 and 2004/2016 World Health Organization Grading Classification Systems in non-muscle-invasive bladder cancer: A European Association of Urology non-muscle invasive bladder cancer guidelines panel systematic review. *Eur. Urol.* **72**, 801–813 (2017).
3. Millán-Rodríguez, F., Chéchile-Toniolo, G., Salvador-Bayarri, J., Palou, J. & Vicente-Rodríguez, J. Multivariate analysis of the prognostic factors of primary superficial bladder cancer. *J. Urol.* **163**, 73–78 (2000).
4. Chang, S. S. *et al.* Treatment of non-metastatic muscle-invasive bladder cancer: AUA/ASCO/ASTRO/SUO guideline. *J. Urol.* **198**, 552–559 (2017).
5. Babjuk, M. *et al.* European Association of Urology Guidelines on non-muscle-invasive bladder cancer (TaT1 and carcinoma in situ)—2019 update. *Eur. Urol.* **76**, 639–657 (2019).
6. Witjes, J. A. *et al.* European Association of Urology Guidelines on muscle-invasive and metastatic bladder cancer: Summary of the 2020 guidelines. *Eur. Urol.* **79**, 82–104 (2021).
7. Cumberbatch, M. G. K. *et al.* Repeat transurethral resection in non-muscle-invasive bladder cancer: A systematic review. *Eur. Urol.* **73**, 925–933 (2018).
8. Panebianco, V. *et al.* Multiparametric magnetic resonance imaging for bladder cancer: Development of VI-RADS (Vesical Imaging-Reporting and Data System). *Eur. Urol.* **74**, 294–306 (2018).
9. Woo, S. *et al.* Diagnostic performance of vesical imaging reporting and data system for the prediction of muscle-invasive bladder cancer: A systematic review and meta-analysis. *Eur. Urol. Oncol.* **3**, 306–315 (2020).
10. Jazayeri, S. B. *et al.* Diagnostic accuracy of vesical imaging-reporting and data system (VI-RADS) in suspected muscle invasive bladder cancer: A systematic review and diagnostic meta-analysis. *Urol. Oncol.* (2021).
11. Aslan, S., Cakir, I. M., Oguz, U., Bekci, T. & Demirelli, E. Comparison of the diagnostic accuracy and validity of biparametric MRI and multiparametric MRI-based VI-RADS scoring in bladder cancer; is contrast material really necessary in detecting muscle invasion?. *Abdom. Radiol. (NY)* **47**, 771–780 (2022).
12. Gmeiner, J., Garstka, N., Helbich, T. H., Shariat, S. F. & Baltzer, P. A. Vesical Imaging Reporting and Data System (VI-RADS): Are the individual MRI sequences equivalent in diagnostic performance of high grade NMIBC and MIBC?. *Eur. J. Radiol.* **142**, 109829 (2021).
13. Elshetry, A. S. F., El-Fawakry, R. M., Hamed, E. M., Metwally, M. I. & Zaid, N. A. Diagnostic accuracy and discriminative power of biparametric versus multiparametric MRI in predicting muscle-invasive bladder cancer. *Eur. J. Radiol.* **151**, 110282 (2022).
14. DelliPizzi, A. *et al.* Bladder cancer: do we need contrast injection for MRI assessment of muscle invasion? A prospective multi-reader VI-RADS approach. *Eur. Radiol.* **31**, 3874–3883 (2021).
15. Sakamoto, K. *et al.* Detection of muscle-invasive bladder cancer on biparametric MRI using vesical imaging-reporting and data system and apparent diffusion coefficient values (VI-RADS/ADC). *Bladder Cancer* **6**, 161–169 (2020).
16. Sim, K. C. & Sung, D. J. Role of magnetic resonance imaging in tumor staging and follow-up for bladder cancer. *Transl. Androl. Urol.* **9**, 2890–2907 (2020).
17. Sobin, L. H., Gospodarowicz, M. K. & Wittekind, C. *TNM Classification of Malignant Tumours* (Wiley, 2011).
18. Zapala, P. *et al.* Clinical rationale and safety of restaging transurethral resection in indication-stratified patients with high-risk non-muscle-invasive bladder cancer. *World J. Surg. Oncol.* **16**, 6 (2018).
19. Ibáñez Muñoz, D. *et al.* Virtual cystoscopy, computed tomography urography and optical cystoscopy for the detection and follow-up for bladder cancer. *Radiologia* **59**, 422–430 (2017).
20. Barchetti, G. *et al.* Multiparametric MRI of the bladder: Inter-observer agreement and accuracy with the Vesical Imaging-Reporting and Data System (VI-RADS) at a single reference center. *Eur. Radiol.* **29**, 5498–5506 (2019).
21. Ueno, Y. *et al.* Diagnostic accuracy and interobserver agreement for the Vesical Imaging-Reporting and Data System for muscle-invasive bladder cancer: A multireader validation study. *Eur. Urol.* **76**, 54–56 (2019).
22. Wang, H. *et al.* Multiparametric MRI for bladder cancer: Validation of VI-RADS for the detection of detrusor muscle invasion. *Radiology* **291**, 668–674 (2019).
23. Del Giudice, F. *et al.* Prospective Assessment of Vesical Imaging Reporting and Data System (VI-RADS) and its clinical impact on the management of high-risk non-muscle-invasive bladder cancer patients candidate for repeated transurethral resection. *Eur. Urol.* **77**, 101–109 (2020).
24. Pecoraro, M. *et al.* Vesical Imaging-Reporting and Data System (VI-RADS) for assessment of response to systemic therapy for bladder cancer: Preliminary report. *Abdom. Radiol. (NY)* **47**, 763–770 (2022).
25. Contieri, R. *et al.* Long-term follow-up and factors associated with active surveillance failure for patients with non-muscle-invasive bladder cancer: The Bladder Cancer Italian Active Surveillance (BIAS) experience. *Eur. Urol. Oncol.* **5**, 251–255 (2022).
26. Fasulo, V. *et al.* Xpert bladder cancer monitor may avoid cystoscopies in patients under “active surveillance” for recurrent bladder cancer (BIAS Project): Longitudinal cohort study. *Front. Oncol.* **12**, 832835. <https://doi.org/10.3389/fonc.2022.832835> (2022).
27. Thoeny, H. C., Bellin, M. F., Comperat, E. M. & Thalmann, G. N. Vesical Imaging-Reporting and Data System (VI-RADS): Added value for management of bladder cancer patients?. *Eur. Urol.* **74**, 307–308 (2018).
28. Leyba, K. & Wagner, B. Gadolinium-based contrast agents: Why nephrologists need to be concerned. *Curr. Opin. Nephrol. Hypertens.* **28**, 154–162 (2019).
29. Mathur, M., Jones, J. R. & Weinreb, J. C. Gadolinium deposition and nephrogenic systemic fibrosis: A radiologist’s primer. *Radiographics* **40**, 153–162 (2020).
30. Costello, J. R., Kalb, B. & Martin, D. R. Incidence and risk factors for gadolinium-based contrast agent immediate reactions. *Top. Magn. Reson. Imaging* **25**, 257–263 (2016).
31. Rose, T. A. Jr. & Choi, J. W. Intravenous imaging contrast media complications: The basics that every clinician needs to know. *Am. J. Med.* **128**, 943–949 (2015).
32. Saita, A. *et al.* Assessing the feasibility and accuracy of high-resolution microultrasound imaging for bladder cancer detection and staging. *Eur. Urol.* **77**, 727–732 (2020).
33. Diana, P. *et al.* Head-to-head comparison between high-resolution microultrasound imaging and multiparametric MRI in detecting and local staging of bladder cancer: The BUS-MISS protocol. *Bladder Cancer* **2022**, 1–9 (2022).
34. Di Campli, E. *et al.* Diagnostic accuracy of biparametric vs multiparametric MRI in clinically significant prostate cancer: Comparison between readers with different experience. *Eur. J. Radiol.* **101**, 17–23 (2018).
35. Noh, T. I. *et al.* Diagnostic accuracy and value of magnetic resonance imaging-ultrasound fusion transperineal targeted and template systematic prostate biopsy based on bi-parametric magnetic resonance imaging. *Cancer Res. Treat.* **52**, 714–721 (2020).
36. Ye, L. *et al.* Biparametric magnetic resonance imaging assessment for detection of muscle-invasive bladder cancer: A systematic review and meta-analysis. *Eur. Radiol.* <https://doi.org/10.1007/s00330-022-08696-5> (2022).
37. Lee, M. *et al.* Non-contrast magnetic resonance imaging for bladder cancer: Fused high b value diffusion-weighted imaging and T2-weighted imaging helps evaluate depth of invasion. *Eur. Radiol.* **27**, 3752–3758 (2017).
38. Lee, C. H., Tan, C. H., Faria, S. C. & Kundra, V. Role of imaging in the local staging of urothelial carcinoma of the bladder. *AJR Am. J. Roentgenol.* **208**, 1193–1205 (2017).
39. Rabie, E., Faeghi, F., Izadpanahi, M. H. & Dayani, M. A. Role of dynamic contrast-enhanced magnetic resonance imaging in staging of bladder cancer. *J. Clin. Diagn. Res.* **10**, Tc01–Tc05 (2016).
40. Scosyrev, E., Noyes, K., Feng, C. & Messing, E. Sex and racial differences in bladder cancer presentation and mortality in the US. *Cancer* **115**, 68–74 (2009).

41. Torres da Costa, E. S. V., Costalonga, E. C., Coelho, F. O., Caires, R. A. & Burdmann, E. A. Assessment of kidney function in patients with cancer. *Adv. Chronic Kidney Dis.* **25**, 49–56 (2018).
42. Barth, B. K. *et al.* Detection of clinically significant prostate cancer: Short dual-pulse sequence versus standard multiparametric MR imaging—A multireader study. *Radiology* **284**, 725–736 (2017).

Acknowledgements

This study was supported by grants from the Korea university College of Medicine.

Author contributions

T.I.N. Protocol/project development, data acquisition, data analysis and interpretation, and drafting the manuscript. J.S.S.: Protocol/project development and supervision. S.G.K.: Protocol/project development and supervision. D.J.S.: Protocol/project development and supervision. J.C.: Protocol/project development and supervision. K.C.S.: Protocol/project development, data acquisition, and supervision. S.H.K.: Protocol/project development, data acquisition, and supervision.

Competing interests

The authors declare no competing interests.

Additional information

Supplementary Information The online version contains supplementary material available at <https://doi.org/10.1038/s41598-022-19273-7>.

Correspondence and requests for materials should be addressed to K.C.S. or S.H.K.

Reprints and permissions information is available at www.nature.com/reprints.

Publisher's note Springer Nature remains neutral with regard to jurisdictional claims in published maps and institutional affiliations.



Open Access This article is licensed under a Creative Commons Attribution 4.0 International License, which permits use, sharing, adaptation, distribution and reproduction in any medium or format, as long as you give appropriate credit to the original author(s) and the source, provide a link to the Creative Commons licence, and indicate if changes were made. The images or other third party material in this article are included in the article's Creative Commons licence, unless indicated otherwise in a credit line to the material. If material is not included in the article's Creative Commons licence and your intended use is not permitted by statutory regulation or exceeds the permitted use, you will need to obtain permission directly from the copyright holder. To view a copy of this licence, visit <http://creativecommons.org/licenses/by/4.0/>.

© The Author(s) 2022